Investigation of Chaotic and Spiking Dynamics in Mid-Infrared Quantum Cascade Lasers Operating Continuous-Waves and Under Current Modulation

Olivier Spitz ⓘ, Jiagui Wu ⓘ, Andreas Herdt, Mathieu Carras, Wolfgang Elsäßer, *Senior Member, IEEE*, Chee-Wei Wong, *Fellow, IEEE*, and Frédéric Grillot, *Senior Member, IEEE*

Abstract—This study investigates chaotic and spiking dynamics of mid-infrared quantum cascade lasers operating under external optical feedback and emitting at 5.5 μm and 9 μm. In order to deepen the understanding, the route to chaos is experimentally studied in the case of continuous-wave and current modulation operation. The non-linear dynamics are analyzed with bifurcation diagrams. While for quasi-continuous wave operation, chaos is found to be more complex, pure continuous wave pumping always leads to the generation of a regular spiking induced low-frequency fluctuations dynamics. In the latter, results show that by combining external optical feedback with periodic forcing and further induced current modulation allows a better control of the chaotic dropouts. This work provides a novel insight into the development of future secure free-space communications based on quantum cascade lasers or unpredictable optical countermeasure systems operating within the two transparency atmospheric windows hence between 3 μm– 5 μm and 8.5 μm–11 μm.

Index Terms—Nonlinear dynamics, external optical feedback, entrainment phenomenon, quantum cascade laser, mid-infrared photonics, secure communications.

I. INTRODUCTION

RECENT progress in the study of non-linear dynamics using delay-coupled semiconductor lasers has paved the way for integrated complex photonics [1], which is becoming a field versatile enough to mimic bioinspired concepts such as neural networks and large-scale synchronization [2]. To this end, triggering spikes in semiconductor lasers has become a field of growing importance with the intent of controlling precisely the time interval and the amplitude of these events. A technique commonly used to achieve such goal is to combine the non-linear effects induced by optical or optomechanical feedback with a bias perturbation. Recent experimental efforts about on-demand extreme events [3], Canard explosions [4] and other non-linear phenomena [5] in semiconductor lasers emphasize a renewed interest in this domain that has been explored both numerically and experimentally since the 90ies [6]–[11]. However, most of these experimental studies have been carried out in the near-infrared region with standard laser diodes governed by interband transitions. In this paper, we report an experimental analysis of the spiking non-linear dynamics in mid-infrared quantum cascade lasers (QCLs) emitting at 5.5 μm and 9.0 μm, the latter being extremely relevant for free-space communications across the atmosphere, because highly transparent between 8.5 μm– 11 μm. Indeed, it is known that turbulence on the propagation path significantly deteriorates the optical signal causing e.g. beam spreading, beam wandering, scintillation or loss of spatial coherence [12]. In this case, the scintillation will be the predominant phenomenon, corresponding to intensity fluctuations of the propagating beam. This effect evolves as a function of $\lambda^{-7/6}$ [13], and will therefore be less significant at higher wavelength hence the advantage of mid-infrared waves for free-space optical communications. QCLs with compact size and improved power efficiency are advantageous compared to large CO_2 lasers with complex setup and high power consumption. In addition, commercial detectors within this optical range are expensive and uncommon, which further increases the cost of eavesdropping and makes mid-infrared QCLs candidates of high potential for free-space communications with enhanced privacy. QCLs are

O. Spitz is with the LTCI Télécom Paris, Institut Polytechnique de Paris, 75013 Paris, France, and with the Fang Lu Mesoscopic Optics and Quantum Electronics Laboratory, University of California Los Angeles, Los Angeles, CA 90095 USA, and also with mirSense, Centre d'intégration NanoInnov, 91120 Palaiseau, France (e-mail: olivier.spitz@telecom-paristech.fr).

J. Wu is with the Fang Lu Mesoscopic Optics and Quantum Electronics Laboratory, University of California Los Angeles, Los Angeles, CA 90095 USA, and also with College of Electronic and Information Engineering, Southwest University, Chongqing 400715, China (e-mail: mgh@swu.edu.cn).

A. Herdt and W. Elsäßer are with the Technische Universität Darmstadt, D-64289 Darmstadt, Germany (e-mail: andreas.herdt@physik.tu-darmstadt.de; elsaesser@physik.tu-darmstadt.de).

M. Carras is with mirSense, Centre d'intégration NanoInnov, 91120 Palaiseau, France (e-mail: mathieu.carras@mirsense.com).

C.-W. Wong is with the Fang Lu Mesoscopic Optics and Quantum Electronics Laboratory, University of California Los Angeles, Los Angeles, CA 90095 USA (e-mail: cheewei.wong@ucla.edu).

F. Grillot is with the LTCI Télécom Paris, Institut Polytechnique de Paris, 75013 Paris, France, and with the Center for High Technology Materials, University of New-Mexico, Albuquerque, NM 87106 USA, and also with the Fang Lu Mesoscopic Optics and Quantum Electronics Laboratory, University of California Los Angeles, Los Angeles, CA 90095 USA (e-mail: frederic.grillot@telecom-paristech.fr).

Color versions of one or more of the figures in this article are available online at http://ieeexplore.ieee.org.

Digital Object Identifier 10.1109/JSTQE.2019.2937445

versatile and powerful optical sources based on intersubband transitions operating not only in the mid-infrared but also in the terahertz domain [14], with optical power over 4.5 W at 4.7 μm in continuous-wave operation at room temperature [15] and an expected power of 20 W with broadband and thermally optimized QCLs [16]. So far, QCLs have been successfully utilized for non-invasive sensing, light detection and ranging (LIDAR) as well as optical countermeasures [17]. Also, due to the broad development of integrated MIR technologies, QCLs on silicon are now highly envisioned as a promising solution for many integrated mid-infrared applications in gas sensing, defense, and medical applications [18], [19]. Finally, recent results about their chaotic behavior under external optical feedback [20] pave the way for free-space secure communications. The combination of optical nonlinearities and ultrafast dynamics is a booming feature and it can give rise to unprecedented physical insights revolutionizing the next generation of quantum cascade devices. External optical feedback consists in reinjecting part of the light emitted by a laser via a mirror thus forming an external cavity. The behavior of the laser is then determined by the amount of optical feedback that couples back into the laser cavity, and which is called the feedback ratio, as well as the phase and the polarization of the back-reflected wave [21]. In laser diodes, the amount of feedback required to destabilize the laser and enter a chaotic state is very low due to a carrier lifetime in the order of the nanoseconds. QCLs exhibit much shorter carrier lifetimes in the order of the picoseconds [22] and therefore, the feedback ratio leading to a chaotic behavior is more important (a few percent). Additionally, very low temperatures seem to facilitate this non-linear process [23]. A particular feature of QCLs is the absence of relaxation oscillations [24], which is a direct consequence of the relatively short carrier lifetime compared to the photon lifetime. To this end, when applying external optical feedback to a QCL pumped with a quasi-continuous bias, the deterministic chaos is characterized by periodic oscillations at the external cavity frequency followed by a low-frequency fluctuation (LFF) pattern leading to dropouts in the experimental time trace [20]. Yet, the time interval between these dropouts is not constant. Adding a direct current modulation with a periodic sine forcing makes the spikes appear for a given phase shift of the external frequency modulation corresponding to the entrainment phenomenon [25], [26].

This paper further investigates the nonlinear dynamical features of a mid-infrared QCL operating under optical feedback with continuous-wave operation and, respectively, current modulation. Section II introduces the features of the QCLs under study emitting at 5.5 μm and 9.0 μm as well as the experimental setup. Section III investigates chaotic dynamics in QCLs operating at room temperature and different pumping conditions. The route to chaos is experimentally studied in the case of a quasi-continuous bias and a continuous bias and the non-linear dynamics are analyzed with bifurcation diagrams. Although chaos with improved reliability and higher dimensionality is obtained with a QCL pumped quasi-continuously, our results anticipate that the subsequent synchronization may be more difficult to be achieved. Section IV investigates the spiking dynamics under current modulation. With continuous bias, the
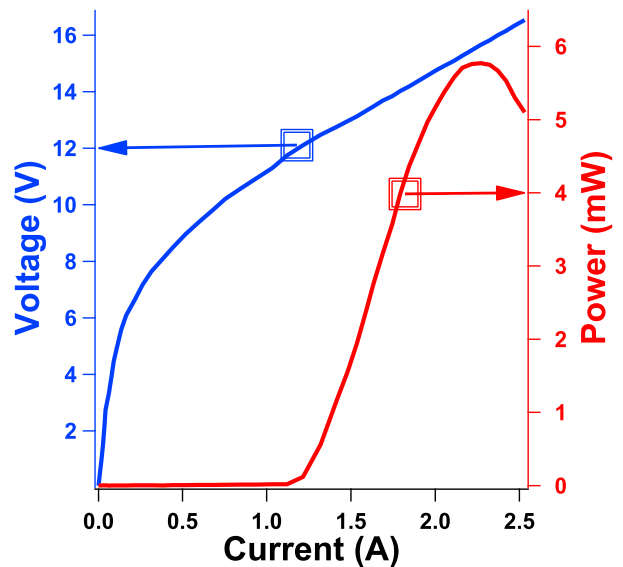

Fig. 1. V-I (blue) and L-I (red) curves of a free-running Type 2 QCL operating at 290K in pulsed operation mode (12% duty cycle at a repetition frequency of 400 kHz).

chaotic pattern displays a LFF induced spiking dynamics. Although this deterministic chaos is of lower dimensionality, it may be promising for developing secure communication links where the chaotic pattern itself can be used to encode information, as described in Section V. Lastly, Section VI summarizes the results and provides conclusions on the work conducted.

II. EXPERIMENTAL APPARATUS

A. Devices

The devices under investigatio are lasers manufactured by mirSense and inspired by the designs described in Ref. [27] and Ref. [28]. These designs allow producing QCLs with wavelengths around 5.5 μm and 9 μm, refer to as Type 1 and Type 2, respectively throughout this study. We have previously reported some results on the performance of Type 1 QCLs where the characteristics of these lasers are fully described [23]. In addition, measurements on the linewidth enhancement factor (more commonly called the α-factor) of such lasers were also carried out. The retrieved above-threshold value of the effective α-factor is in the order of 2 whereas for currents below threshold, it is in the order of -0.4 [29], [30]. This relatively large enhancement of the linewidth enhancement factor can be attributed to the QCLs operation far above the threshold current and to the distributed feedback grating cavity which can induce severe longitudinal spatial hole burning [31].

The LIV characteristics and the optical spectrum of a Type 2 QCL are depicted in Fig. 1 and Fig. 2, respectively. The QCLs under study are equipped with a distributed feedback (DFB) grating, which means that they emit single mode at the aforementioned wavelengths. The whole structure of Type 1 QCLs is epi-side down mounted which allows some of the Type 1 lasers to be pumped with a continuous bias for temperature up to 313 K. This type of QCLs can also be cooled down to cryogenic
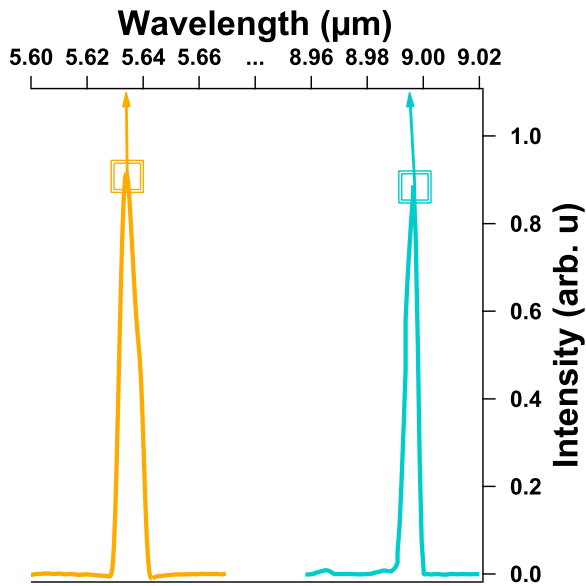
Fig. 2. Experimental spectrum of a free-running Type 1 QCL (orange) and Type 2 QCL (cyan) operating at 290 K with pulses of 300 ns with a repetition frequency of 400 kHz (representing a 12% duty cycle).

temperature, allowing us to carry out a feedback-sensitivity analysis with respect to the temperature for a range of more than 200 K [23]. In the case of Type 2 QCLs, the lasers are in an epi-side up configuration and require temperatures below 65 K to be pumped with a continuous current. The experiment was carried out at 40 K with a liquid helium cooling. The threshold current of Type 1 QCLs is in the range of 250–350 mA with a continuous bias and liquid nitrogen cooling. For Type 2 QCLs, the threshold with continuous bias and liquid helium cooling is in the range of 900–1100 mA.

B. Experimental Setup

The QCLs under study are inserted inside a cryostat or, for some QCLs of Type 1, in a ILX LDM 4872 QCL mount which allows working conditions between 248 K and 313 K. Due to the highly divergent beams, a focusing mid-infrared lens is placed in front of the QCL. The external cavity, which is realized by the emitting facet of the QCL and the gold-plated mirror, results in external optical feedback and a polarizer allows controlling the amount of feedback. Setting it to $90°$, corresponding to a TM polarization, leads to a maximum feedback ratio. The beam is completely blocked when the polarizer is set to $0°$. Thanks to a non-polarizing beam splitter (NPBS), part of the QCL's beam can be analyzed with a fast oscilloscope and real time spectrum analyzer (RSA). The detector used is a Mercury-Cadmium-Telluride detector (MCT) and the signal retrieved by this detector is amplified with a low-noise amplifier. The QCL is powered with a low-noise current source (Wavelength Electronics QCL2000 LAB) which provides the continuous current. This current source has a built-in low-pass filter and is designed to be modulated up to 3 MHz with a sine modulation and up to 2 MHz with a square modulation. We implement the modulation with a waveform generator (Rigol DG1022Z) at 200 mega samples

per second. We were able to experimentally reach modulation frequencies up to 5 MHz in the case of a sine modulation but the amplitude of the modulation strongly decreases due to the 3 MHz bandwidth of the current source. Regarding all aforementioned bandwidth requirements, we focus on frequencies below 1 MHz to be able to carry out a relevant comparison between the case where a sine modulation is added and the case where a square modulation is used.

III. Room Temperature Quasi-Continuous Wave and Continuous Wave Chaotic Dynamics

A. Quasi-Continuous Wave

In this section, we focus on the observation of non-linear phenomena when the operation temperature is close to 290 K. When varying the amount of external optical feedback by means of the mid-infrared polarizer, several regimes such as stable operation and LFF appear. These phenomena have been already found and described in the case of quasi-continuous bias, both close to room temperature [20] and cryogenic temperature [23]. Studying these non-linear phenomena in the case of a continuous bias is essential for practical applications of such lasers into a communication system, however, it requires the optical path to be very stable. Indeed, as detailed in the next section, the frequency of the current modulation is one of the main components of the RF spectrum, both in the case of a sine and square modulation. Consequently, it seems likely that the LFF phenomenon builds up on a frequency determined by the modulation frequency. This cannot happen in the case of a continuous bias because no specific frequencies are a priori fostered. The experiments are consequently carried only with Type 1 QCLs within a LDM 4872 mount, because this configuration provides less vibrations than the one using a cryostat and a vacuum pump. It can be assured that feedback is at its maximum when the amplitude of the spikes, described in the next section, is also at its maximum. It is important to emphasize that the symmetry of the pattern needs to be carefully retrieved. Indeed, restabilization can occur in semiconductor laser with external optical feedback [32], meaning that the feedback can lead to a case where the signal is constant and the RF spectrum is flat. We actually never observed such a behavior in the case of a quasi-continuous bias. Being able to precisely assess the golden mirror tilt giving the maximum feedback ratio leads to phenomena which are highly reproducible.

Fig. 4A) shows a selection of experimental time traces when varying the feedback ratio from 0% to the achievable maximum of 24.6% for a quasi-continuous bias with a pulse width of $2 \mu s$. The lowest value of feedback strength displays a stable signal corresponding to free-running operation. Oscillations start appearing for feedback ratios above 1.1% and the transition between oscillations and the LFF regime can be observed for a feedback ratio of 2%. The deterministic pattern becomes then more complex until the maximum feedback ratio of 24% is obtained. The related bifurcation diagram is plotted in Fig. 4B) and displays the extrema of the experimental time traces for a selection of feedback strengths. Increasing the feedback ratio lead to changes in the dynamics observed in the time traces. The
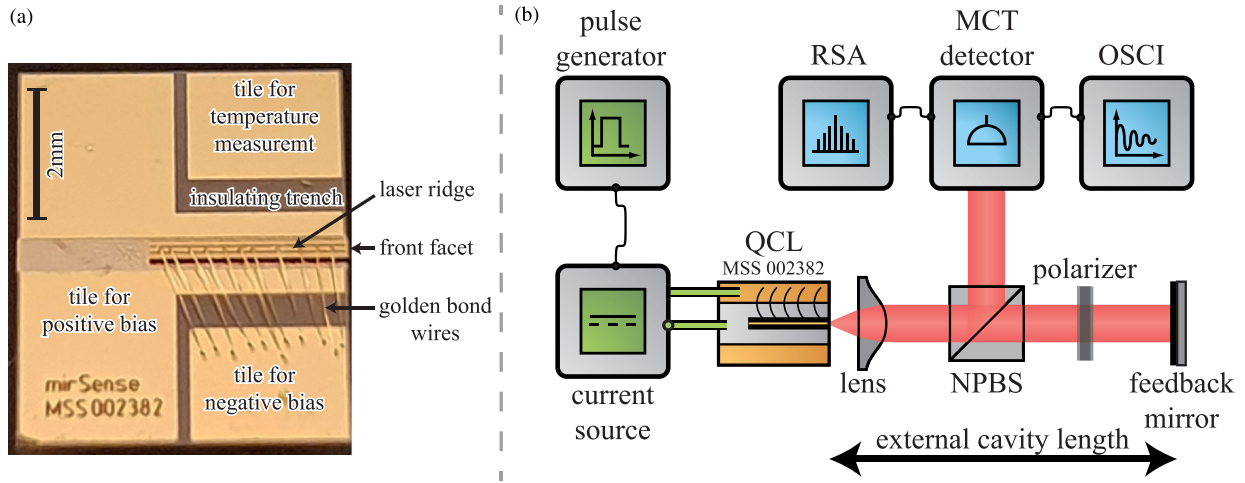
Fig. 3. Close-up of a Type 2 QCL (a) and experimental setup (b) with an external cavity length for the conventional optical feedback; NBPS: non-polarizing beam splitter, MCT: Mercury-Cadmium-Telluride detector, OSCI: fast oscilloscope, RSA: real-time spectrum analyzer.
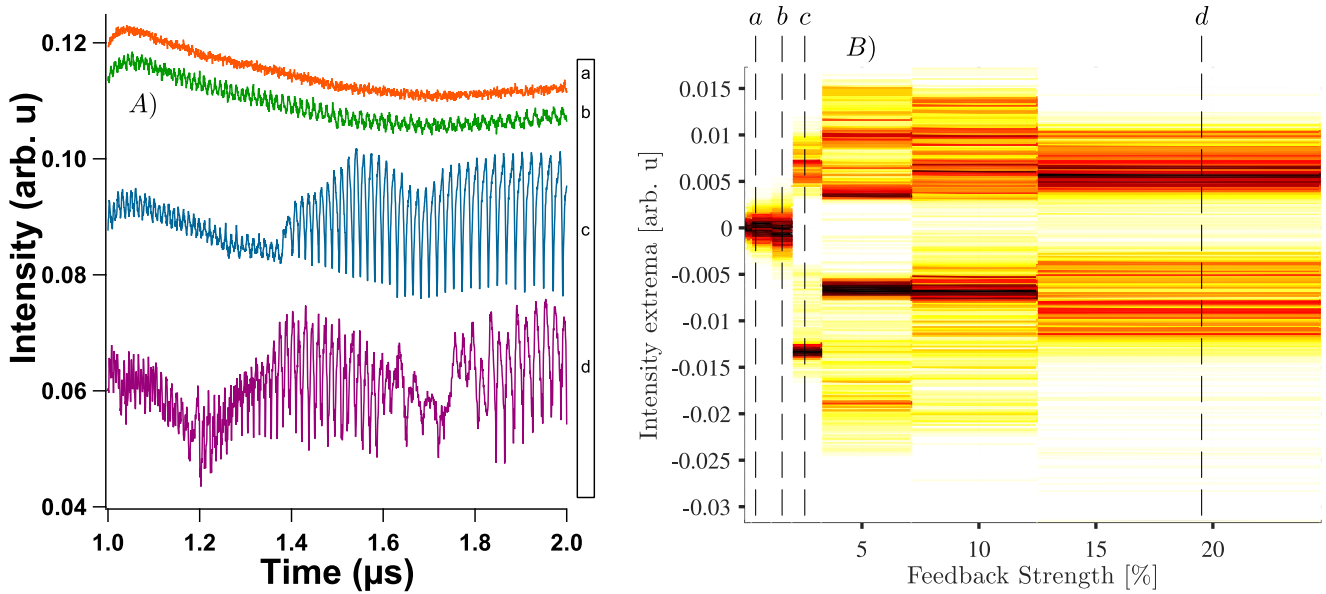

Fig. 4. Experimental time traces when the laser is pumped in the quasi-continuous mode (A) for several values of the feedback strength in % and related bifurcation diagram (B) when the temperature is 290 K. a) 0.05%, b) 1.1%, c) 3.3%, d) 24.6%; For low feedback strength, the signal is nearly continuous and then, with increasing feedback strength, evolves towards non-linear patterns such as oscillations and LFF.

dashed lines correspond to the different feedback strengths at the far-right of the solid lines, but are placed in the middle of the solid lines for visual guidance for the reader and represent the analysis of the time traces of Fig. 4A). The bifurcation diagram plotted in Fig. 4B) shows a Hopf bifurcation for a feedback strength of 3.3%. The corresponding time-periodic oscillations for higher feedback ratios have a frequency of nearly 50 MHz, which is ten times lower than the theoretical frequency of the external cavity ($f_{ext} \approx 430$ MHz) when oscillations are expected to occur [20]. This behavior may be due to multiple reflections since the laser is operated at $I = 2.2 \times I_{th}$, which corresponds to the current leading to the maximum output power. Figure 5 shows that the external cavity frequency is missing for a configuration close

to the Hopf bifurcation. Yet, this figure demonstrates that the frequency of the external cavity can be found in the LFF pattern for high feedback ratios, as already reported in Ref. [23] for a feedback ratio of 24%. When increasing feedback strength above 3.3%, the intensity extrema spread over a wide range of values corresponding to the onset of a chaotic pulsing output combined with fast pulses, which is represented by solid lines around the zero intensity value in the bifurcation diagram. A numerical model of a QCL under similar conditions and a simulation of the bifurcation diagram can be found in Ref. [20]. It is worth noticing that the simulated bifurcation diagram displays the same route to chaos but for higher feedback strengths. In that experimental configuration, the transition between the oscillations and the
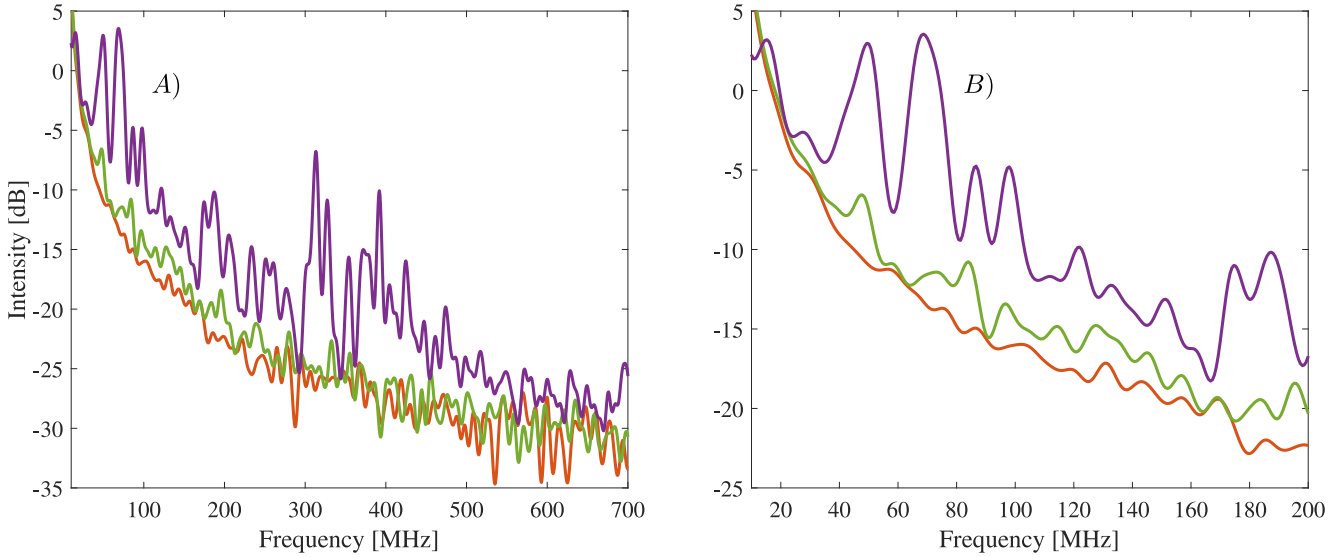
Fig. 5. RF spectra related to Fig. 4a), b) and d) and obtained with a Fast Fourier Transform (colors remain the same). (A) analysis of the whole bandwidth. Only the purple curve (corresponding to a high feedback strength) shows the contribution of the external cavity frequency around 330 MHz. A small discrepancy between the theoretical cavity frequency and the experimental one has already been pointed out [20], [23]. (B) Close-up on low frequencies, the green curve (low feedback strength) is characterized by small bumps around 42 and 86 MHz, contrary to the orange curve (zero feedback strength). This supports the claim that the frequency of the pattern seen in Fig. 4b) may be related to multiple reflections in the external cavity.
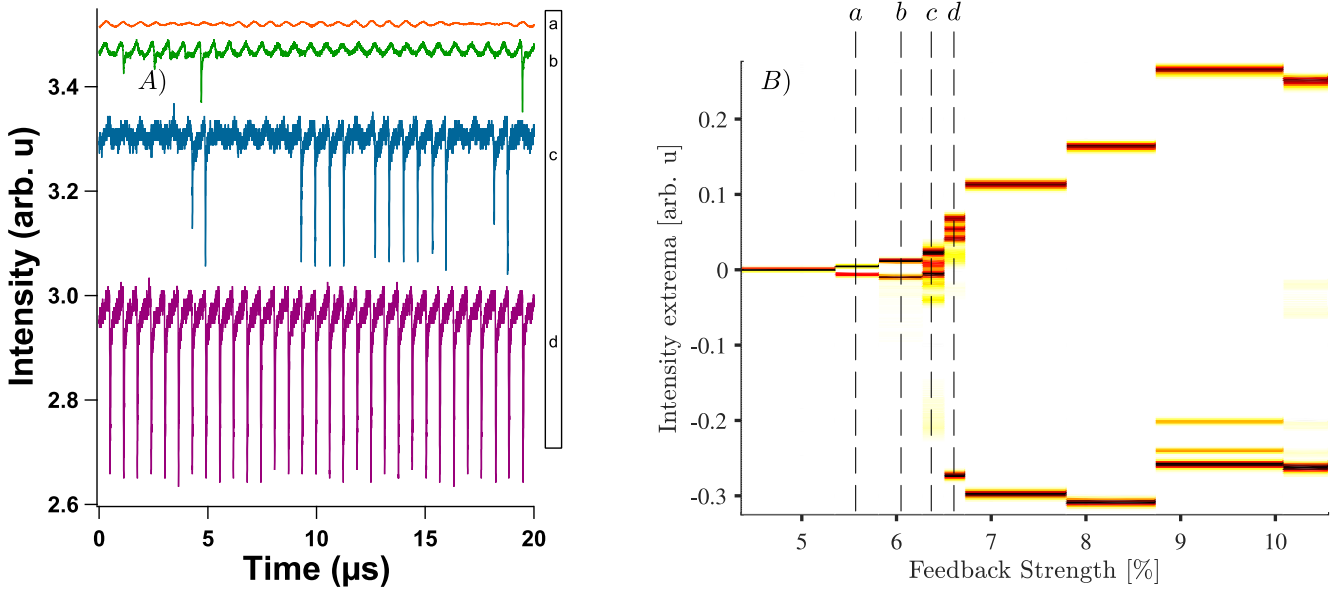

Fig. 6. Experimental time traces in continuous mode (A) for several values of the feedback strength in % and related bifurcation diagram (B) when the temperature is 249 K. a) 5.81%, b) 6.27%, c) 6.50%, d) 6.72%; The signal is primarily steady and then evolves to non-linear patterns such as oscillations and LFF. Traces b) and c) show the transition between an oscillatory state and the LFF regime, when the periodic pattern starts displaying dropouts with high amplitude. For feedback strength below 5%, the QCL's signal is constant.

LFF regime is characterized by the coexistence of the two regimes as shown in Fig. 4A), plot c).

B. Continuous Wave

For the experiments with a pure continuous bias, a QCL from the same batch as the one used for the quasi-continuous wave experiments was utilized. This means that the two lasers are made with the same epitaxial stacks but tiny defects in the growing process make them slightly different : the previous one

can only be pumped with a 70% duty cycle at 263 K whereas the laser we are going to focus on now can be pumped with a continuous bias. Fig. 6A) and Fig. 7A) show the evolution of the time traces when increasing the feedback strength at two different temperatures where several non-linear patterns can be experimentally observed. The LFF pattern is better visualized in Fig. 6A) while Fig. 7A) displays a restabilization. The changes in the retrieved waveforms might be due to the intrinsic definition of chaotic behavior for which a tiny change in the initial conditions can lead to very different results [33]. For instance,
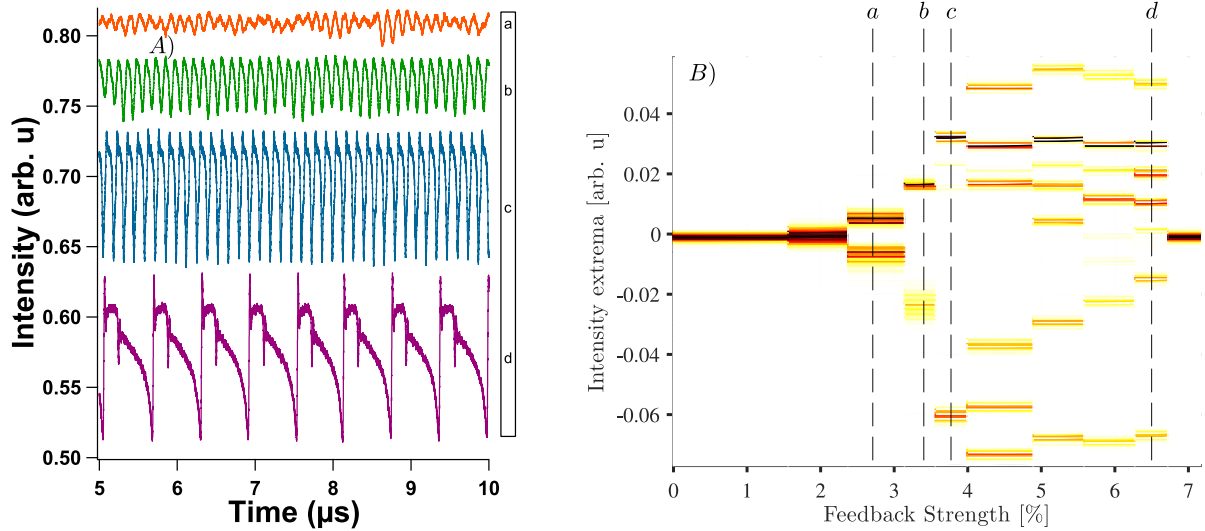
Fig. 7.　Experimental time traces for continuous operation (A) for several values of the feedback strength in % and related bifurcation diagram (B) when the temperature is 263 K. a) 3.14%, b) 3.56%, c) 3.99%, d) 6.72%; values above 7.16% lead to a stable signal and this corresponds to a restabilization, which is never seen in the case of a quasi-continuous bias. Traces a) and b) exhibit several extrema and could be of prime interest in the case of secure communications through chaos synchronization.

the transition between oscillations and the LFF pattern can be clearly seen in Fig. 6A) : some dropouts start appearing for a feedback ratio of 6.27% and then become the preponderant pattern above 6.50% (compare Fig. 6A) plot b) with plot c)). In the case of Fig. 7A), the transition does not look the same. The amplitude of the oscillations increases to give a chaotic pattern with several maxima and minima (Fig. 7A, plots c) and d)) before an homogenization of the extrema and the occurring of a pattern similar to the LFF dynamics already studied [23]. It is also worth noticing that the LFF pattern in the case of Fig. 7A) has the same curvature than the LFF pattern studied in [23], which is not the case of the LFF pattern of Fig. 6A). Indeed, the latter exhibits a slow increase before a sudden drop related to the competition between modes which is expected from this type of lasers under perturbation [32]. Albeit different in shape, the two observed patterns were retrieved for an identical configuration, except the temperature of the heat sink. Further investigations are needed to determine which parameters could change the curvature of the LFF. The bifurcation diagrams (Fig. 6B) and Fig. 7B)) are also quite different from the one obtained in the quasi-continuous case. Both show a Hopf bifurcation point but then, the route to chaos only displays a limited number of extrema, except for the transition between the oscillatory and the LFF state. In the continuous bias case, we have never observed fast oscillations at the frequency of the external cavity though the pump current is highly above threshold ($I = 1.7 \times I_{th}$ for the continuous bias experiments). This is the reason why the bifurcation diagrams do not show solid lines around the value corresponding to a constant output of the laser, and whose ordinate is 0 in the bifurcation diagram. For one of the two configurations, we were able to see a restabilization for feedback ratios larger than 7.2%, until the maximum achievable feedback ratio of 10.5%. Depicted time traces in Fig. 7A) also display, in the middle of each LFF pattern, a singular notch for the highest values of feedback ratio

(see Fig. 7A), plot d)). This leads to another splitting in the bifurcation diagram because in that case, not only one minimum and one maximum exist. For the same range of feedback ratios, the global pattern is very similar and the frequency of this pattern decreases from 4 MHz to 1.5 MHz before the signal becomes stable again with the restabilization shown in Fig. 7B). Another difference between the quasi-continuous and the continuous case is the characteristic time of the non-linear dynamics. For the continuous case, the characteristic time is around 1 μs with a continuous bias (which is equivalent to a quasi-continuous bias with an infinite period) and it goes down below 0.1 μs when the laser is pumped with a quasi continuous bias with a pulse width of 2 μs. For pulse widths below 1 μs, the QCL remains in a transient state and it is difficult to study the non-linear dynamics. This discrepancy may be due to a sum of non-linear, electrical and thermal effects in the quasi-continuous case.

All these facts show that QCLs can be used in secure communications through chaos synchronization because these semiconductor lasers exhibit a wide diversity of non-linear dynamics and a slight change in the initial experimental conditions can lead to various patterns. This is especially true for continuous bias, when no specific frequencies (except the one of the external cavity) are injected into the system, which further complicate the deciphering of the encoded message for a third party. If a synchronization can be achieved, methods already demonstrated with laser diodes [34], [35] could be implemented in QCLs for free-space transmissions.

IV. SPIKING DYNAMICS UNDER CURRENT MODULATION

Applying both an external optical feedback and current modulation allows synchronizing the spikes of the LFF with the frequency of the forcing. This is the entrainment phenomenon, already mentioned in the introduction. Most of the studies focus
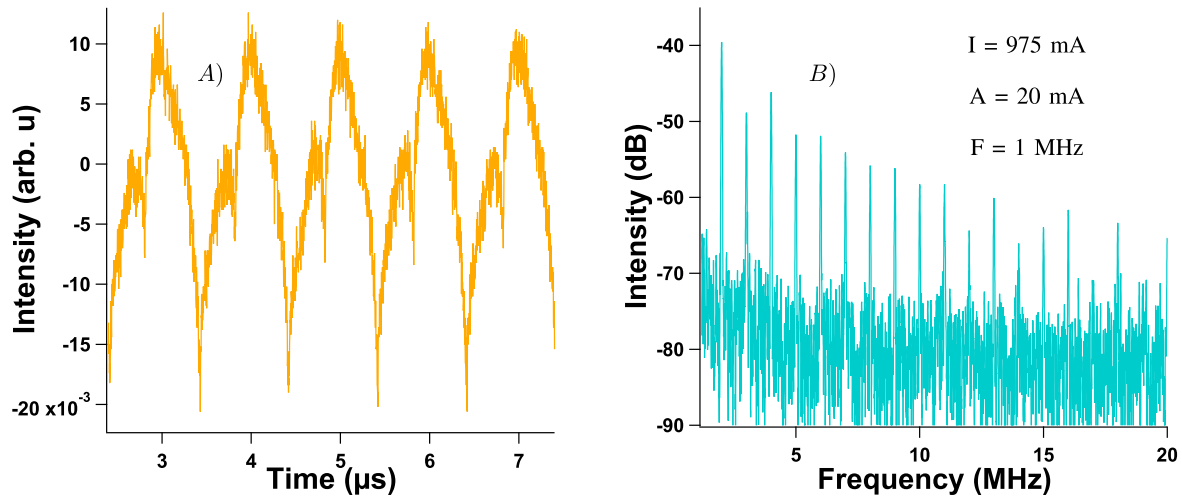
Fig. 8. Experimental time trace (A) and RF spectrum (B) when external optical feedback and a sine modulation at 1 MHz with an amplitude of 2% is applied. The RF spectrum starts at a frequency of 1.2 MHz to visualize the significant frequencies. I: continuous pump current, A: peak-to-peak amplitude of the modulation, F: frequency of the modulation.
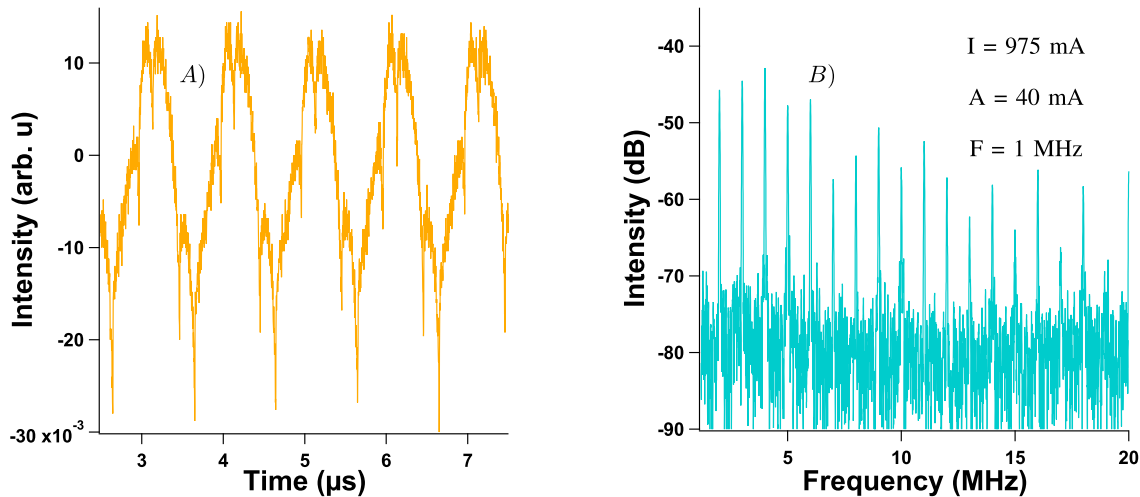

Fig. 9. Experimental time trace (A) and RF spectrum (B) when external optical feedback and a sine modulation at 1 MHz with an amplitude of 4% is applied. The RF spectrum starts at a frequency of 1.2 MHz to visualize the significant frequencies. I: continuous pump current, A: peak-to-peak amplitude of the modulation, F: frequency of the modulation.

on a sine wave modulation that is applied to the laser, the latter being moreover pumped with a continuous current above threshold. Here, we study both the case of a sine wave modulation and the case of a square wave modulation. A square wave modulation is not identical to a quasi-continuous wave in the sense that a continuous bias is applied prior to the addition of the square wave modulation. A quasi-continuous bias starts well below threshold and goes up to the required value of bias current. Most of the time, the starting point is at a few dozens of mA because when remaining too close to zero mA, the voltage is quite unstable and this can also lead to a voltage slope that is beyond the required specification of the current source, especially in a cryogenic environment where LIV characteristics are highly sensitive to temperature [36]. For the sine wave modulation case, we focus on the Type 2 QCL whose wavelength is very relevant for free-space communication purposes [37]. These are, to the best of our knowledge, the first results reporting on the non-linear dynamics

of QCLs emitting right in the transparency window between 8.5 μm and 11 μm. Similar results with a Type 1 QCL have already been reported [38]. Fig. 8A) shows the synchronization of the LFF spikes with the sine wave modulation. The continuous bias applied to the QCL is 975 mA and a sine modulation with an amplitude of 20 mA (2% of the pump current) and a frequency of 1 MHz is applied. In this case, there are two dropouts per periods, always occurring for the same phase shift of the periodic forcing. Fig. 8B) displays the RF spectrum retrieved with the RSA. It is composed of several spikes with a constant frequency interval of 1 MHz, corresponding to the frequency of the sine wave modulation. The entrainment phenomenon is however not only defined by the frequency of the modulation. For instance, Fig. 9A) shows the time trace under the conditions described in Fig. 8, except that the sine wave modulation has now an amplitude of 40 mA (4% of the pump current). The synchronization with the periodic forcing still occurs but the number of dropouts per
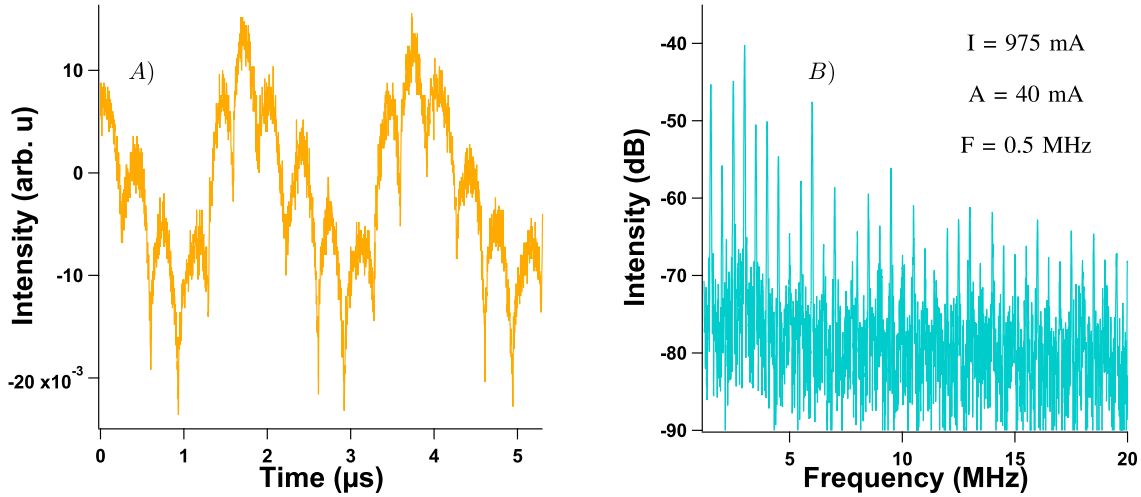
Fig. 10. Experimental time trace (A) and RF spectrum (B) when external optical feedback and a sine modulation at 0.5 MHz with an amplitude of 4% is applied. The RF spectrum starts at a frequency of 1.2 MHz to visualize the significant frequencies. I: continuous pump current, A: peak-to-peak amplitude of the modulation, F: frequency of the modulation.
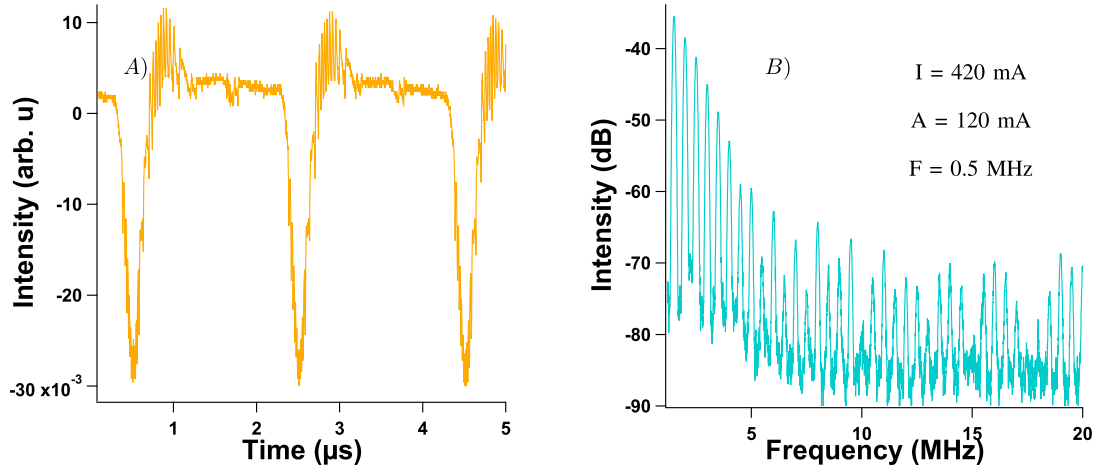

Fig. 11. Experimental time trace (A) and RF spectrum (B) when external optical feedback and a square wave modulation at 0.5 MHz with an amplitude of 28% is applied. The RF spectrum starts at a frequency of 1.2 MHz to visualize the significant frequencies. I: continuous pump current, A: peak-to-peak amplitude of the modulation, F: frequency of the modulation.

period doubles. This main change in the waveform has nevertheless very small impact on the RF spectrum analysis. Fig. 9B) shows that the spectrum is still composed of spikes which are separated by 1 MHz. A decrease in the forcing frequency leads also to a decrease in the intervals that are retrieved in the RF spectrum. Fig. 10B) displays the RF spectrum in the case where the frequency of the sine wave is 0.5 MHz and its amplitude is 40 mA. And indeed, the frequency interval between spikes is 0.5 MHz. Fig. 10A) shows that the number of dropouts per period has also changed. It is consequently possible to tune the number of spikes per period when the LFF spikes are entrained by varying either the frequency or the amplitude of the applied forcing. The higher the frequency, the lower the number of spikes and the lower the amplitude, the lower the number of spikes. Other results with a Type 1 QCL showed that the value of the continuous pump that is applied prior to the periodic modulation has very small influence on the number of spikes per period [38]. If the periodic forcing is not a sine wave but a square wave, like

shown in Fig. 11A), the conclusions remain similar for the RF spectrum analysis. In the case of a Type 1 QCL, Fig. 11B) shows that the frequency interval is 0.5 MHz when the bias forcing is a square wave with a frequency of 0.5 MHz and a duty cycle of 90%. The shape of the spikes in the spectrum looks however a bit different compared to Fig. 10B) but this is only due to the frequency step that was chosen to carry out the analysis with the RSA. The time trace also displays a synchronization of the LFF dropouts as seen in Fig. 11A). Dropouts always appear for a given phase shift of the square signal, especially along the slopes of the square. But contrary to the cases with a sine wave modulation, the time interval between the dropouts is not constant anymore. Dropouts are mainly gathered at the upper edge of the square and are seldom in the plateau region corresponding to the constant value of the upper part of the square. It is worth noticing that despite the similarities of the RF spectra regardless of the kind of forcing used and the dependence on the frequency of the modulation, the dropouts synchronize

with the forcing in several ways. This observation could lead to a very precise triggering of such dropouts and can be highly relevant for secure communications.

V. CONCLUSION

This work addresses a comprehensive investigation of chaotic and spiking dynamics in mid-infrared QCLs operating under continuous-waves and current modulation. In particular, the study unveils for the first time dynamical results with a QCL emitting at 9 μm. Overall, results show that depending on the pumping conditions, QCLs can exhibit different routes to chaos. On the one hand, when using quasi-continuous wave operation, chaos is found to be more complex, which could be very advantageous for secure communications purposes. Secure communication is achieved via a master and a slave laser with similar parameters and operating conditions in order to allow the synchronization [39]. The master laser is chaotically driven with external control methods (e.g. optical injection, optical feedback), then synchronized with the slave laser, and eventually, the message to be transmitted is hidden inside the chaotic signal of the master laser [40]. The decoding is divided into two steps: a detector records the signal (with the encrypted message) from the master laser and another detector records the one from the slave laser, which is a mirror image of the master's chaos. Substracting the intensities of the first detector with that of the second detector allows recovering the hidden message [41]. However, synchronization may be difficult to achieve in the case of quasi-continuous pumping, because the thermal shift inside the laser's structure leads to a shift in the emission wavelength of the QCL. On the other hand, pure continuous wave pumping leads to a more regular spiking dynamics that can be controlled by adding current modulation. This entrainment phenomenon studied by adding sine and square wave modulations allows finely triggering the spiking that is suitable for secure communications where the chaos itself contains the secret message [42]. Moreover, developed chaos can also be found in this configuration for narrow ranges of feedback ratios. Even if these specific spots can be difficult to reach, they can be candidates of choice for chaos synchronization and secure communications because the temperature of the device remains steady. In summary, this work is of paramount importance for the development of compact secure high-speed communication systems in the mid-infrared domain. The findings of this study can be implemented in applications ranging from civil to defense with a focus on airborne communications, spaceborne communications (such as transmissions between satellites or transmissions between space rovers) and last-mile connections in remote or devastated areas. Further studies will now concentrate on the chaos synchronization as well as on the implementation of a private QCL transmission channel operating at high-speed.

ACKNOWLEDGMENT

REFERENCES

[1] M. C. Soriano, J. García-Ojalvo, C. R. Mirasso, and I. Fischer, "Complex photonics: Dynamics and applications of delay-coupled semiconductors lasers," *Rev. Modern Phys.*, vol. 85, no. 1, pp. 421–470, 2013.

[2] J. Zamora-Munt, C. Masoller, J. Garcia-Ojalvo, and R. Roy, "Crowd synchrony and quorum sensing in delay-coupled lasers," *Phys. Rev. Lett.*, vol. 105, no. 26, 2010. Art. no. 264101.

[3] T. Jin, C. Siyu, and C. Masoller, "Generation of extreme pulses on demand in semiconductor lasers with optical injection," *Opt. Express*, vol. 25, no. 25, pp. 31 326–31 336, 2017.

[4] F. Marino, M. Ciszak, S. Abdalah, K. Al-Naimee, R. Meucci, and F. Arecchi, "Mixed-mode oscillations via canard explosions in light-emitting diodes with optoelectronic feedback," *Phys. Rev. E*, vol. 84, no. 4, 2011, Art. no. 047201.

[5] C. Quintero-Quiroz, J. Tiana-Alsina, J. Romà, M. Torrent, and C. Masoller, "Quantitative identification of dynamical transitions in a semiconductor laser with optical feedback," *Sci. Rep.*, vol. 6, 2016, Art. no. 37510.

[6] J. Mork, B. Tromborg, and J. Mark, "Chaos in semiconductor lasers with optical feedback: Theory and experiment," *IEEE J. Quantum Electron.*, vol. 28, no. 1, pp. 93–108, Jan. 1992.

[7] J. Sacher, D. Baums, P. Panknin, W. Elsäßer, and E. O. Göbel, "Intensity instabilities of semiconductor lasers under current modulation, external light injection, and delayed feedback," *Phys. Rev. A*, vol. 45, no. 3, pp. 1893–1905, 1992.

[8] I. Fischer, G. Van Tartwijk, A. Levine, W. Elsäßer, E. Göbel, and D. Lenstra, "Fast pulsing and chaotic itinerancy with a drift in the coherence collapse of semiconductor lasers," *Phys. Rev. Lett.*, vol. 76, no. 2, pp. 220–223, 1996.

[9] T. Heil, I. Fischer, and W. Elsäßer, "Influence of amplitude-phase coupling on the dynamics of semiconductor lasers subject to optical feedback," *Phys. Rev. A*, vol. 60, no. 1, pp. 634–641, 1999.

[10] D. W. Sukow and D. J. Gauthier, "Entraining power-dropout events in an external-cavity semiconductor laser using weak modulation of the injection current," *IEEE J. Quantum Electron.*, vol. 36, no. 2, pp. 175–183, Feb. 2000.

[11] I. Fischer, Y. Liu, and P. Davis, "Synchronization of chaotic semiconductor laser dynamics on subnanosecond time scales and its potential for chaos communication," *Phys. Rev. A*, vol. 62, no. 1, 2000, Art. no. 011801.

[12] A. Delga and L. Leviandier, "Free-space optical communications with quantum cascade lasers," in *Proc. Quantum Sens. Nano Electron. Photon. XVI*, 2019, Art. no. 1092617.

[13] A. K. Majumdar and J. C. Ricklin, *Free-Space Laser Communications: Principles and Advances*, vol. 2. Berlin, Germany: Springer, 2010.

[14] M. S. Vitiello, G. Scalari, B. Williams, and P. De Natale, "Quantum cascade lasers: 20 years of challenges," *Opt. Express*, vol. 23, no. 4, pp. 5167–5182, 2015.

[15] A. Lyakh, R. Maulini, A. Tsekoun, R. Go, and C. K. N. Patel, "Tapered 4.7 μm quantum cascade lasers with highly strained active region composition delivering over 4.5 watts of continuous wave optical power," *Opt. Express.*, vol. 20, no. 4, pp. 4382–4388, 2012.

[16] M. Suttinger, R. Go, P. Figueiredo, and A. Lyakh, "Towards 20-watt continuous wave quantum cascade lasers," in *Proc. Micro Nanotechnol. Sensors, Syst., Appl. X*, 2018, Art. no. 1063922.

[17] R. J. Grasso, "Defence and security applications of quantum cascade lasers," in *Proc. Opt. Sens., Imag., Photon Counting, Nanostructured Devices Appl.*, 2016, Art. no. 99330F.

[18] A. Spott *et al.*, "Quantum cascade laser on silicon," *Optica*, vol. 3, no. 5, pp. 545–551, 2016.

[19] A. Spott, E. J. Stanton, N. Volet, J. D. Peters, J. R. Meyer, and J. E. Bowers, "Heterogeneous integration for mid-infrared silicon photonics," *IEEE J. Sel. Topics Quantum Electron.*, vol. 23, no. 6, pp. 1–10, Nov./Dec. 2017.

[20] L. Jumpertz, K. Schires, M. Carras, M. Sciamanna, and F. Grillot, "Chaotic light at mid-infrared wavelength," *Light, Sci. Appl.*, vol. 5, no. 6, 2016, Art. no. e16088.

[21] A. Gavrielides *et al.*, "Square-wave self-modulation in diode lasers with polarization-rotated optical feedback," *Opt. Lett.*, vol. 31, no. 13, pp. 2006–2008, 2006.

[22] M. A. Talukder and C. R. Menyuk, "Temperature-dependent coherent carrier transport in quantum cascade lasers," *J. Phys.*, vol. 13, no. 8, 2011, Art. no. 083027.

[23] O. Spitz, J. Wu, M. Carras, C.-W. Wong, and F. Grillot, "Low-frequency fluctuations of a mid-infrared quantum cascade laser operating at cryogenic temperatures," *Laser Phys. Lett.*, vol. 15, no. 11, 2018, Art. no. 116201.

[24] R. Paiella *et al.*, "High-frequency modulation without the relaxation oscillation resonance in quantum cascade lasers," *Appl. Phys. Lett.*, vol. 79, no. 16, pp. 2526–2528, 2001.

[25] T. Sorrentino, C. Quintero-Quiroz, M. Torrent, and C. Masoller, "Analysis of the spike rate and spike correlations in modulated semiconductor lasers with optical feedback," *IEEE J. Sel. Topics Quantum Electron.*, vol. 21, no. 6, Nov./Dec. 2015, Art. no. 1801107.

[26] J. Tiana-Alsina, C. Quintero-Quiroz, M. Panozzo, M. Torrent, and C. Masoller, "Experimental study of modulation waveforms for entraining the spikes emitted by a semiconductor laser with optical feedback," *Opt. Express*, vol. 26, no. 7, pp. 9298–9309, 2018.

[27] J. Yu, S. Slivken, A. Evans, J. David, and M. Razeghi, "Very high average power at room temperature from $\lambda \approx 5.9\,\mu$ m quantum-cascade lasers," *Appl. Phys. Lett.*, vol. 82, no. 20, pp. 3397–3399, 2003.

[28] S. Slivken, Z. Huang, A. Evans, and M. Razeghi, "High-power ($\lambda \sim 9\,\mu$ m) quantum cascade lasers," *Appl. Phys. Lett.*, vol. 80, no. 22, pp. 4091–4093, 2002.

[29] L. Jumpertz *et al.*, "Measurements of the linewidth enhancement factor of mid-infrared quantum cascade lasers by different optical feedback techniques," *AIP Adv.*, vol. 6, no. 1, 2016, Art. no. 015212.

[30] O. Spitz, A. Herdt, J. Duan, M. Carras, W. Elsäßer, and F. Grillot, "Extensive study of the linewidth enhancement factor of a distributed feedback quantum cascade laser at ultra-low temperature," in *Quantum Sensing Nano Electron. Photon. XVI, Int. Soc. Opt. Photon.*, vol. 10926, 2019, Art. no. 1092619.

[31] A. Gordon *et al.*, "Multimode regimes in quantum cascade lasers: From coherent instabilities to spatial hole burning," *Phys. Rev. A*, vol. 77, no. 5, 2008, Art. no. 053804.

[32] L. Jumpertz, *Nonlinear Photonics in Mid-Infrared Quantum Cascade Lasers*. Berlin, Germany: Springer, 2017.

[33] E. N. Lorenz, *The Essence of Chaos*. Seattle, WA, USA: University of Washington Press, 1995.

[34] G. D. Vanwiggeren and R. Roy, "Communication with chaotic lasers," *Science*, vol. 279, no. 5354, pp. 1198–1200, 1998.

[35] A. Argyris *et al.*, "Chaos-based communications at high bit rates using commercial fibre-optic links," *Nature*, vol. 438, no. 7066, pp. 343–346, 2005.

[36] R. Terazzi, T. Gresch, M. Giovannini, N. Hoyler, N. Sekine, and J. Faist, "Bloch gain in quantum cascade lasers," *Nature Phys.*, vol. 3, no. 5, pp. 329–333, 2007.

[37] S. Blaser, D. Hofstetter, M. Beck, and J. Faist, "Free-space optical data link using Peltier-cooled quantum cascade laser," *Electron. Lett.*, vol. 37, no. 12, pp. 778–780, 2001.

[38] O. Spitz, J. Wu, M. Carras, C.-W. Wong, and F. Grillot, "Chaotic optical power dropouts driven by low frequency bias forcing in a mid-infrared quantum cascade laser," *Sci. Rep.*, vol. 9, no. 1, 2019, Art. no. 4451.

[39] M. Sciamanna and K. A. Shore, "Physics and applications of laser diode chaos," *Nature Photon.*, vol. 9, no. 3, pp. 151–162, 2015.

[40] C. R. Mirasso, P. Colet, and P. García-Fernández, "Synchronization of chaotic semiconductor lasers: Application to encoded communications," *IEEE Photon. Technol. Lett.*, vol. 8, no. 2, pp. 299–301, Feb. 1996.

[41] P. Colet and R. Roy, "Digital communication with synchronized chaotic lasers," *Opt. Lett.*, vol. 19, no. 24, pp. 2056–2058, 1994.

[42] S. Hayes, C. Grebogi, and E. Ott, "Communicating with chaos," *Phys. Rev. Lett.*, vol. 70, no. 20, pp. 3031–3034, 1993.

Olivier Spitz was born in Besançon, France, on June 2, 1991. He received the Diplôme d'Ingénieur degree in physics, from the École Supérieure de Physique et de Chimie Industrielles, Paris, France, and from the Institut d'Optique Graduate School, Palaiseau, France. He also received the french examination called "Agrégation" in physics in 2016, which is a national examination for the recruitment of teachers at high school and undergraduate level. He is currently working toward the Ph.D. degree with Télécom ParisTech, Paris, France working on the non-linear dynamics of quantum cascade lasers under external optical feedback or injection and has been a Visiting Scholar with the Electrical Engineering and Computer Science Department, University of California Los Angeles, Los Angeles, USA, between September 2017 and March 2018.

Jiagui Wu was born in Sichuan, China, in 1981. He received the B.Sc. degree in physics and the M.Sc. degree in optics from Southwest University, Chongqing, China, in 2003 and 2006, respectively, and the Ph.D. degree in non-linear dynamics from Sichuan University, Chengdu, China, in 2014. He is a Professor with the College of Electronic and Information Engineering, Southwest University, and a Visiting Scholar with the Electrical Engineering and Computer Science Department, University of California Los Angeles, Los Angeles, USA. He has authored or coauthored more than 60 publications including about 40 journal papers. His current research interests include the nonlinear dynamics of semiconductor lasers, chaos generation and synchronization in microcavities, and chaos secure communications.

Andreas Herdt was born in Wetzlar, Germany, on June 19, 1991. He received the B.Sc. and M.Sc. degrees in physics from the Technical University of Darmstadt, Darmstadt, Germany, in 2014 and 2016, respectively. In 2017, he was awarded with the "Green Photonics Award for Young Academic Researchers" from Fraunhofer IOF for the work of his master's thesis. He is currently working with the group of Prof. Elsäßer (Technical University of Darmstadt) toward the Ph.D. degree.

Mathieu Carras was born in France in 1979. He received the Ph.D. degree in solid-state physics from the University of Paris VII, Denis Diderot, France, in 2006. He then joined the III-V Laboratory with Alcatel Thales, Palaiseau, France, as a permanent Research Staff Member working on modeling, design, and characterization of quantum cascade lasers. He is especially involved in electron transport and electromagnetics. His interests include mid-infrared and far-infrared quantum cascade lasers and quantum infrared detectors (QWIPs and quantum cascade detectors). He is currently the CEO of mirSense, the company he founded in 2014, after being the Head of the team developing mid-infrared lasers at the III-V Laboratory.

Wolfgang Elsäßer (M'94–SM'98) was born in Pforzheim, Germany, in 1954. He received the Diploma in physics from Karlsruhe Technical University, Karlsruhe, Germany, in 1980, the Ph.D. degree in physics from the University of Stuttgart, Stuttgart, Germany, in 1984, and the Habilitation degree in experimental physics from the Philipps University of Marburg, Marburg, Germany, in 1991. He was with the Max Planck Institute for Solid State Research, Stuttgart, from 1981 to 1985. From 1985 to 1995, he was with the Philipps University of Marburg. Since 1995, he has been a Professor with the Institute of Applied Physics, Technische Universität Darmstadt, Darmstadt, Germany, where he is currently the Head of the Semiconductor Optics Group. He is a member of the German Physical Society and the European Physical Society. He was the recipient of the Otto Hahn Medal in 1985, the Werner von Siemens Medal in 1985, the Rudolf Kaiser Prize in 1991, the IEE J. J. Thomson Premium in 1995, the Hassia Cooperation Award in 2004, and the Darmstadt Technology Transfer Foundation Award in 2011.

Chee-Wei Wong received the double B.Sc. degree and B.A. degree with highest distinction from the University of California at Berkeley, Berkeley, CA, USA, in 1996 and 1999, respectively. He received the Masters of Science and Doctorate of Science degrees from the Massachusetts Institute of Technology, Cambridge, MA, USA, in 2001 and 2003, respectively. He is a Faculty Member with the University of California, Berkeley, CA, USA and, prior to that, a Tenured Faculty Member with Columbia University, New York City, NY, USA. He is elected a Fellow of SPIE, OSA, ASME, and the recipient of the 2018 NIH Early Scientist Trailblazer Award, DARPA Young Faculty Award, NSF CAREER Award, Google Faculty Award, and 3M Faculty Award among others. He is also a finalist in the Qualcomm Innovation Award, Maiman Award, and holds visiting professorships with the Chinese Academy of Sciences and the Nanyang Technological University. His work has appeared in more than 290 journals and conferences, including *Nature, Science Advances, Physical Review Letters, Nature Physics, Nature Photonics, Nature Communications, Nature—Light: Science & Applications* series among others. He delivered more than one hundred plenary and invited talks at universities and industry, published four book chapters, and has been awarded 19 patents and 11 provisional patents. He has supervised 27 Ph.D. students and research scientists, more than half are now in their own professorships including full professors, and sat on 75 Ph.D. thesis committees.

Frédéric Grillot was born in Versailles, France, on August 22, 1974. He received the M.Sc. degree in physics from the University of Dijon, Dijon, France, in 1999, the Ph.D. degree in electrical engineering from the University of Besançon, Besançon, France, in 2003, and the Research Habilitation in physics from the University of Paris VII, Paris, France, in 2012. His doctoral research activities were conducted within the optical component research department with Nokia Bell Labs (formerly Alcatel-Lucent) working on the effects of the optical feedback dynamics in semiconductor lasers, and the impact this phenomenon has on communication systems. From 2003 to 2004, he was with the Center for Nanoscience and Nanotechnology (C2N) at the Université Paris-Saclay where he focused on integrated optics modeling and silicon-based passive devices for optical interconnects. Between 2004 and 2012, he used to be an Assistant Professor with the Institut National des Sciences Appliquées, Rennes, France. From 2008 to 2009, he was a Visiting Research Professor with the University of New-Mexico, Albuquerque, USA leading research in optoelectronics at the Center for High Technology Materials. In October 2012, he joined Télécom Paris, one of the top public institutions of higher education and research of engineering in France as an Associate Professor and became a Full Professor in January 2017. Since August 2015, he has also been serving as a Research Professor with the University of New-Mexico. During April–December 2017, he joined the Electrical Engineering Department with the University of California Los Angeles, USA as a Visiting Professor teaching dynamics of lasers and applied quantum mechanics. He has authored 90 journal articles, one book, three book chapters, and more than 200 contributions in international conferences and workshops. His current research interests include, but are not limited to, advanced quantum confined devices using new materials such as quantum dots and dashes, light emitters based on intersubband transitions, nonlinear dynamics and optical chaos in semiconductor lasers systems as well as microwave and silicon photonics applications. He is currently an Associate Editor for *Optics Express* and a Senior Consultant for Advisor Technology Partnerships at Baehl Innovation. He is a Fellow Member of the SPIE, a Senior Member of the IEEE Photonics Society, and a Senior Member of the OSA.